3D seismic survey design optimization

Gijs J.O. Vermeer, 3DSymSam – Geophysical Advice

In 3D seismic survey design, the parameter choice has to satisfy a wide variety of geophysical, operational and cost constraints. The designer of a survey has to strike a balance between the various requirements and invariably he will have to settle for some kind of compromise. Hence, this design process could also be viewed as an optimization process.

In an award-winning poster paper Liner et al. (1998) introduced the idea of survey design optimization. It was soon followed by another poster paper, but now in The Leading Edge (Liner et al., 1999). The method described in Liner, Underwood, and Gobeli (1999; to be called the LUG method in this paper) honors geophysical requirements only. This method determines design parameters based on the minimization of a cost function that is a weighted sum of deviations from the user-specified geophysical target values.

Morris, Kenyon and Beckett (2001) introduced a different survey design optimization method (to be called the MKB method). The MKB method focuses on the minimization of the actual cost of a 3D survey, while satisfying a number of geophysical constraints. The geophysical constraints can be formulated according to the same geophysical requirements as used in the LUG method. In the MKB method the cost function is minimized using the Solver function available in Microsoft Excel.

The MKB method as well as the LUG method serve as inspiration for this paper in which I will present modifications and improvements to both methods. The published methods deal with orthogonal geometry and so does this paper. To optimize the optimization method a clear understanding of what constitutes a geophysically desirable configuration is essential. Therefore, this paper starts with a description of the main parameters of orthogonal geometry and their interrelationships. Next, various geophysical requirements that may influence the choice of the geometry parameters are reviewed. Then the LUG method and the MKB method will be reviewed, followed by modifications of the MKB method and the LUG method. The modified methods will be illustrated with some examples of 3D survey design.

Description of orthogonal geometry. Figure 1 illustrates the dual description of regular orthogonal geometry. The left side of the picture shows the way in which the data may be acquired in the field, whereas the right side shows that the acquisition geometry may also be described in terms of cross-spreads. (The geometry might also be acquired with cross-spreads but that would be highly inefficient.)

The range of shots in the template defines the crossline roll of the geometry. In Figure 1 the shot range equals one receiver line interval leading to a one-line roll. This type of rolling ensures that all cross-spreads are the same with the receiver line cutting the spread of shots in the center (except along the edges of the survey). If the range of shots equals several receiver line intervals, say 3, then the crossline roll will be equal to 3. In that case 3 different cross-spreads will be acquired with differences between the positive and negative maximum cross-line offsets. Although those multi-line roll acquisition geometries would produce constant fold at deep levels (where no offset muting is applied), they would show strong fold variations causing severe acquisition footprints at intermediate levels (see also Vermeer, 2002, Section 4.6.6). One-line roll geometries show much less variation in fold at intermediate levels. Therefore, like in the MKB and LUG methods, I will only optimize for one-line roll.

The width of the midpoint area of the cross-spread equals half the length of the receiver spread (see Figure 1). It is also equal to the maximum inline offset $X_{\max,i}$. Similarly, the height of the midpoint area of the cross-spread equals half the length of the shot spread, and this height is also equal to the maximum crossline offset $X_{\max,x}$. The midpoint area of the next cross-spread in the inline direction is shifted over one shot line interval in that direction. Therefore, to create constant inline fold M_i, the shot line interval *SLI* should fit an integer number of times on the width of the cross-spread. Similarly, constant crossline fold M_x is achieved by selecting a receiver line interval *RLI* that fits an integer number of times on the crossline dimension of the cross-spread.

Figure 1 also shows the unit cell of the geometry. Its area equals *RLI* * *SLI*. This area fits $M_i * M_x$ times on the area of the cross-spread, i.e., total fold $M = M_i * M_x$ = (midpoint area of cross-spread) / (area of unit cell). In Figure 1 total fold equals 4 * 4 = 16.

A one-line roll orthogonal geometry is defined by six parameters only. They are listed in Table 1. n_S, n_R, M_i, and M_x are integers. ΔS and ΔR have to fit an integer number n_S and n_R on the receiver line interval and the shot line interval, respectively, to ensure that inline roll and crossline roll distances involve moving an integer number of station spacings. So, any optimization process has to find four integers and two station spacings to define a geometry that will satisfy all geophysical requirements.

Pairwise, the six parameters in Table 1 define the three characteristic aspect ratios of the geometry: the aspect ratio of the bins $A_b = \Delta S / \Delta R$, the aspect ratio of the unit cell $A_u = RLI / SLI$, and the aspect ratio of the cross-spread $A_c = X_{\max,x} / X_{\max,i}$.

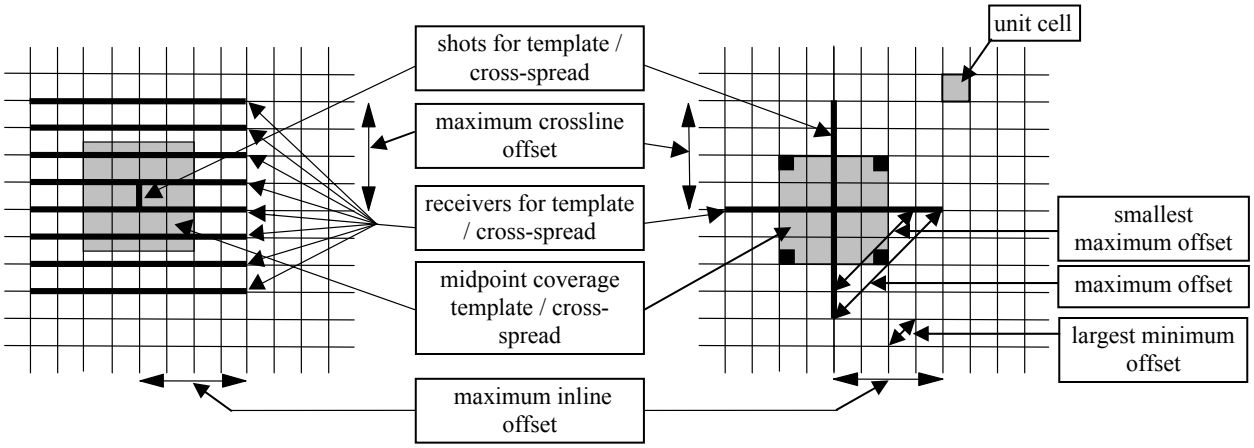

Figure 1. The same orthogonal geometry with template (left) and with cross-spread (right). Horizontal lines are receiver lines; vertical lines are source lines. The template represents the way in which the data may be acquired in the field; in this case there are 8 receiver lines with a number of shots in the center of the template. The cross-spread gathers all data for receivers along the same receiver line that have listened to a range of shots along the same source line (after Vermeer, 2002).

Table 1 Parameters describing regular orthogonal geometry

Receiver station spacing	ΔR
Shot station spacing	ΔS
Receiver line interval	$RLI = n_S * \Delta S$
Shot line interval	$SLI = n_R * \Delta R$
Maximum inline offset	$X_{max,i} = M_i * SLI$
Maximum crossline offset	$X_{max,x} = M_x * RLI$

Geophysical requirements. Figure 1 describes a fully symmetric geometry with all aspect ratios equal to 1. From a physical point of view this constitutes the ideal situation, because physically, there is no difference between properties in the inline direction and in the crossline direction. In particular the receiver sampling interval ΔR along the receiver line and the shot sampling interval ΔS along the shot line should be the same and small enough for proper sampling of the cross-spread. Proper sampling means that the underlying continuous wavefield can be fully reconstructed from the sampled wavefield. Only in case of oversampling, the sampling intervals of inline and crossline direction might be different. Similarly to Morrice et al. (2001) I will use the requirement of equal station spacings in the optimization procedure. [Liner et al., (1999), allow different shot and receiver station spacings.]

Ideally, the aspect ratios of the unit cell and of the cross-spread should be equal to one as well. A square unit cell is better than a rectangular unit cell for a number of reasons. One reason is that the unit cell acts as the basis of offset-vector tile (OVT) gathers (see Vermeer, 2002). In Figure 1 the cross-spread consists of 16 different unit cells. Taking the same cell (tile) from all cross-spreads of the geometry produces a single-fold OVT-gather. Such a gather is the nearest one can get in orthogonal geometry to a common-offset vector (COV) gather. The inevitable variation in offset in an OVT-gather is smallest for square OVTs. Gesbert (2002) and Vermeer (2002) describe the use of those gathers in prestack migration.

Vermeer (2002) also describes that offset-vector oriented muting can achieve constant fold at each time level in the 3D survey, thus minimizing acquisition footprint. This muting procedure is based on splitting each cross-spread in $4M$ quarter-unit-cell sized rectangles. The procedure is most efficient for square unit cells as Figure 2 illustrates. This figure compares geometries 1 and 2 having the same total fold M, and the same square cross-spread as the basic subset. Geometry 1 has $M_i = M_x = 6$, and geometry 2 has $M_i = 4$ and $M_x = 9$. In case no offset-vector oriented muting is applied, fold at each time level will vary, and the variation in fold will be largest for the geometry with rectangular unit cells. A rule of thumb would be to choose at most a factor two difference between shot line interval and receiver line interval.

The desirability of $A_c = 1$ is quite obvious. All traces in a cross-spread with the same absolute offset are lying on a circle with its midpoint at the cross-spread center. Hence, the maximum useful offset is also defined by a circle, and this leads to $X_{max,x} = X_{max,i}$. Assuming equal shot and receiver station spacings, a square cross-spread produces common receiver gathers that are common shot gather look-alikes with the same number of traces. 3D velocity filtering (Galibert et al., 2002; Girard et al., 2002; Karagůl and Crawford, 2003)

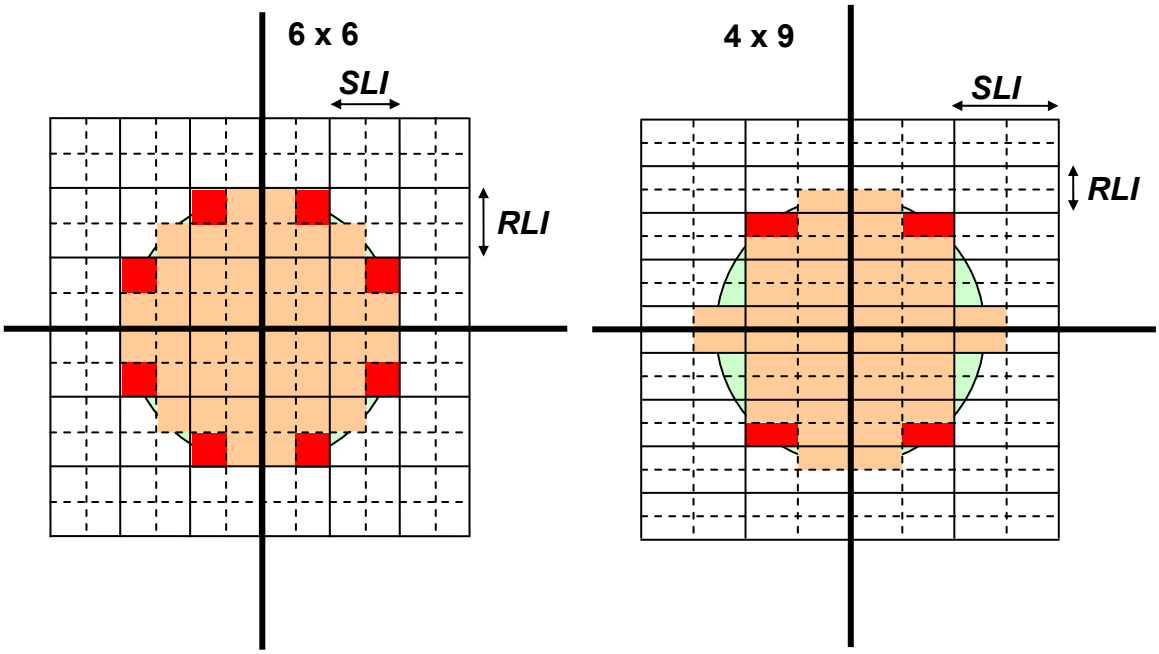

*Figure 2. Offset-vector oriented muting in two 36-fold acquisition geometries. In both geometries $X_{max,i} = X_{max,x} = 1800$ m. Both cross-spreads are split into 4 * 36 = 144 quarter-unit-cell sized areas. Left: SLI = RLI = 300 m, right: SLI = 450 m, RLI = 200 m. All traces in the eight red squares on the left have the same range of absolute offsets (424 m), and all traces of the four red rectangles on the right have another but equal range of absolute offsets (492 m). Assigning the same mute time to all traces in each red square removes the variation in fold that would exist by application of an absolute-offset mute function. At the assigned mute time the fold jumps from integer 11 to integer 13. The same procedure on the right lets the fold jump from 11 to 12. The smaller the range of offsets in each little tile, the better all traces in the tile can be approximated with a single mute time. On the right this offset range is largest.*

stands the best chance of success in square cross-spreads. Another benefit of $A_c = 1$ is that it maximizes the useful extent of the cross-spread in both inline and crossline direction, thus minimizing the number of cross-spread edges for a given fold. The fewer the edges the smaller the impact of migration artifacts caused by spatial discontinuities. In practice, other considerations - mainly cost – may lead to $A_c \neq 1$. Again, a good rule of thumb might be $0.5 < A_c < 2$. Another, slightly more complex, rule might be to require that the ground roll be covered entirely by the cross-spread for optimum removal by 3D velocity filtering.

AVO requirements may need the use of very long offsets, which one would not be interested in for the other objective of structural imaging. In a dual objective situation one may use a much larger maximum inline offset than maximum crossline offset to satisfy AVO requirements. For structural imaging, the long offsets may be discarded to obtain a squarish geometry.

Apart from these basic parameters, there may be quite a few other parameters for which a desirable value can be specified. These other parameters may be total fold M, fold at shallow target F_{sh}, fold at deep target F_{dp}, maximum stretch factor, maximum offset $X_{\max}$, smallest maximum offset $X_{\max\min}$, and largest minimum offset $X_{\min}$.

The designer may have a fairly good idea of the total fold needed. Following the ideal symmetry requirements, the choice of total fold is rather restricted: only squares satisfy this requirement. However, by allowing A_c and A_u to deviate from 1, also other total folds can be achieved. If one allows $n(n + 1)$ in addition to n^2, the choice becomes quite a bit less restricted: 25, 30, 36, 42, 49, etc.

At shallower levels where not all offsets contribute due to muting, the average fold will be smaller than total fold. In general, the fold at shallow targets may be smaller than at deep targets, and the designer may specify average fold as needed at various target levels. The average fold at a shallow target F_{sh} for a given geometry and given mute offset X_{sh} at that level may be computed using simple geometrical relations. Total fold $M = M_i * M_x = X_{\max,i} / SLI * X_{\max,x} / RLI =$ (area of cross-spread) / (area of unit cell). The right-hand side of Figure 1 illustrates this formula for a 16-fold geometry. If muting restricts the range of offsets that contributes, the average fold M_{av} can be computed from M_{av} = (area of cross-spread not muted) / (area of unit cell), see Figure 3.

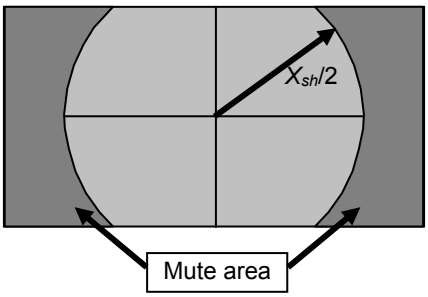

Figure 3. Average fold computed from mute offset and midpoint area of cross-spread. The mute offset X_{sh} cuts a circular area with radius X_{sh} /2 from the midpoint area of a cross-spread. The (truncated) circular area covers all traces that contribute to average fold at the level of the shallow target. In case of offset-vector oriented muting (Figure 2), the circular area is approximated by small squares, and fold is constant.

Note that in this computation use is made of continuous geometry, i.e., areas are measured rather than number of traces in bins. If the sampling intervals are not too large, there will not be much difference between the two computational techniques, but using continuous geometry (infinitely small sampling intervals) facilitates the computations considerably.

The mute offset at various target levels is determined from the mute function. This function is often computed from the velocity function and the maximum allowable NMO stretch factor. In the optimization procedure discussed later, it is assumed that mute offsets at target levels have been determined beforehand.

The parameters maximum offset $X_{\max}$, smallest maximum offset $X_{\max\min}$ and largest minimum offset $X_{\min}$ can also be determined in a simple way using continuous geometry. This is illustrated in the cross-spread of Figure 1. If we take all quarter-unit-cell sized areas in the corners of all cross-spreads of the geometry (black squares in Figure 1), single-fold coverage is constructed containing the largest available offsets in the geometry. The smallest of these largest offsets $X_{\max\min}$ can be found from the corners closest to the center of the cross-spread. $X_{\max\min}$ may play a role in AVO analysis. It could be chosen as the smallest offset needed in all CMPs to cover the required range of angles of incidence. $X_{\min}$ determines the shallowest level where at least complete single-fold coverage is reached.

The LUG optimization method. Having established the requirements of all geophysical parameters as discussed in the previous section, the designer has to determine an acquisition geometry that satisfies all requirements in an optimal way. This can be quite a challenge, and therefore Liner et al. (1998, 1999) devised an optimization technique for survey parameter design (the LUG method).

Liner et al. (1999) also used the fact that regular orthogonal geometry can be described by six parameters. Next to shot and receiver intervals in x and y (corresponding to the first four parameters in Table 1) they used number of live receivers in x- and y-direction rather than maximum inline offset and maximum crossline offset.

In the LUG method a cost function is minimized by using the six parameters as decision variables. The cost function describes deviations from desired values in the following way:

$$Cost = \sum_i w_i \left(\frac{p_i - \mathrm{D}p_i}{p_i} \right)^2 + w_j \left(\frac{t_x - t_y}{t_x + t_y} \right)^2, \qquad (1)$$

p_i is a geophysical parameter, $\mathrm{D}p_i$ its target (desired) value, and w_i a weight attached to parameter p_i. t_x and t_y describe the x- and y-dimension of the template, respectively. Various geophysical parameters used in the LUG method are binsize b_x in x and b_y in y, total fold M, number of available channels, and maximum offset $X_{\max}$. The template term in (1) describes the desirability of a square template. In Liner et al. (1999) t_x and t_y were computed as distances between first and last sample rather than as effective length, i.e., (n – 1) Δ rather than nΔ. As a consequence, maximum offset expressed as $X_{\max} = 0.5\sqrt{(t_x^2 + t_y^2)}$ did not get the correct value.

Liner et al. (1999) first tried a minimization technique available in Mathematica, but to overcome various problems with that technique a special program was written in C to establish from all possible solutions (84 million cases were tested) the one that minimizes the geophysical cost function. However, the number of possible solutions can be reduced significantly by selecting ΔR, ΔS, n_S, n_R, M_i and M_x (see Table 1) as the six parameters to be established. The simplified problem formulation can be solved easily using the Solver function available in MS Office program Excel in a similar way as in Morrice et al. (2001).

The MKB optimization method. The LUG method only optimizes for geophysical parameter requirements. The $€£cost of the acquisition is another important decision factor, and Morrice et al. (2001) formulated the survey design optimization problem as a minimization problem for the $€£cost subject to geophysical and operational constraints (the MKB method).

The cost function includes such things as permitting cost, surveying cost, cutting and clearing cost, drilling cost, daily cost of the crew, and more. For a detailed description see Morrice et al. (2001). The number of decision variables in the MKB method is no less than 13. Two of those are “number of receiver channels moved per day” and “number of shots per day”. Obviously, these two variables are part of the cost computation. However, for any choice of geometry parameters, these two parameters are dependent on each other. Also the other decision parameters appear to be

interdependent and it turns out that my modified MKB method can be formulated with five independent decision variables only (assuming fixed station spacings for shots and receivers).

The constraints in the MKB method are formulated as Left Hand Side (LHS) ≤ Right Hand Side (RHS) or as LHS ≥ RHS. For instance one constraint is $X_{max} \geq \Delta X_{max}$. Other constraints specify that certain variables can only be integers. All this is fed to the Excel Solver, which finds a solution for the optimization problem.

Modified MKB method. The MKB method and the spreadsheet given in Morrice et al. (2001) are used as a starting point. The cost function and cost elements were not changed, but I introduced some significant improvements to the rest of the problem description and solution. First, the number of decision variables is reduced from thirteen to five: n_S, n_R, M_i, M_x, (see Table 1) and "number of shots per day". The first four decision variables are constrained to be integer; implicitly this makes total fold M integer as well, which was not so in the original MKB method. The "number of shots per day" is now allowed to be non-integer, as it concerns a variable that may vary from day to day.

The number of constraints following the LHS ≤ RHS rule has been reduced from sixteen to nine. Currently, there are constraints for X_{min}, X_{max}, F_{sh} (fold at shallow target), F_{dp} (fold at deep target), aspect ratios A_c and A_u, "number of receiver channels", "number of shots per day", and "number of receiver channels moved per day".

X_{min} is constrained as $(X_{min} - \Delta X_{min}) / \Delta X_{min} \leq fraction$, where *fraction* is a positive number representing a maximally allowed relative deviation. Thus X_{min} is not allowed to be much larger than the desired value, but it may be smaller.

The constraints for X_{max}, F_{sh}, and F_{dp} recognize uncertainty attached to target values by allowing negative as well as positive deviations from the target value, e.g., $|(X_{max} - \Delta X_{max})| / \Delta X_{max} \leq fraction$.

The constraints for the aspect ratios A_c and A_u are formulated as Max $(A, 1/A) \leq A_{max}$, where A_{max} is the maximum aspect ratio considered acceptable.

The last three constraints are numbers that are limited to some known maximum.

Modified LUG method. The use of Excel Solver in the LUG method provides interesting additional scope to find optimal designs in an expedient way. All constraints used in the MKB method can also be used in the LUG method (except the constraints on shots per day and receivers per day that influence $€£cost only), whereas some of the constraints on geophysical requirements can be given extra weight by including them in the cost function.

The cost function used in the modified LUG method is

$$Cost = \sum_i w_i \left(\frac{p_i - \Delta p_i}{\Delta p_i} \right)^2, \qquad (2)$$

where currently parameters X_{min}, A_c, A_u, F_{sh} and F_{dp} are included in the list of parameters to be optimized. Of course, $\Delta A_c = \Delta A_u = 1$. Dependent on the type of problem, many other choices of parameters would be possible as well.

Examples. It is interesting and useful to try both optimization methods for the same problem. I will compare the results from the two methods for two different examples.

Example 1 is similar to the problem used as an illustration in Morrice et al. (2001). Some parameters of interest are listed in Table 2. The rows above the heavy line indicate some given and some target values. Below the heavy line, parameters as found with the LUG and MKB methods are listed in columns marked LUG-1 and MKB. Both methods found parameters with $X_{min} < \Delta X_{min}$. The shotline interval *SLI* is much larger in the MKB solution than in the LUG solution. This difference is caused by the MKB method trying to minimize $€£cost with shots being more expensive than receivers, whereas the LUG method puts more emphasis on trying to produce an aspect ratio of the unit cell close to one. The solution given in the LUG-2 column illustrates that interchanging inline and crossline does not make any difference for the LUG method: geophysically the LUG-1 and the LUG-2 solutions are entirely equivalent. However, the MKB cost is lower for the LUG-2 solution than for the LUG-1 solution.

Example 2 is derived from the problem tackled by five different designers at the 1999 EAGE Workshop on 3D seismic surveys (Hornman et al., 2000). In this example the shallowest target is much deeper than in the first example and the required folds are larger (see Table 2). The first solution found with the LUG method (LUG-a) is fully symmetric, thus minimizing the contribution of the two aspect ratios to the LUG cost. Solution MKB-a is asymmetric, again because it wants to minimize the number of expensive shots. However, in both solutions the total fold deviates perhaps more than desirable from the target fold. Imposing a tighter constraint on F_{dp} leads to the solutions specified in columns LUG-b and MKB-b. The rows labeled "LUG cost" and "MKB cost" illustrate the relative trade-off between geophysical requirements and budget constraints.

The formula used to compute average fold for a given mute offset and geometry can be applied to the whole time range provided the mute offset is known as a function of time. Figure 4 compares the average fold as a function of two-way time for the four designs of Example 2. For mute offset $X_{mute} < X_{max,i}$ and $X_{mute} < X_{max,x}$, the average fold is completely determined by X_{mute} and the area of the unit cell, i.e., the line intervals. This is the reason why LUG-a (which has the

smallest unit cell) has the largest average fold at shallow levels.

Table 2 Comparison of LUG and MKB solutions to two different problems

	Example 1 (Morrice)			Example 2 (EAGE)			
	LUG-1	**LUG-2**	**MKB**	**LUG-a**	**LUG-b**	**MKB-a**	**MKB-b**
Station spacings	50 m	50 m	50 m	40 m	40 m	40 m	40 m
Mute offset shallow	1250 m	1250 m	1250 m	2303 m	2303 m	2303 m	2303 m
Mute offset deep	2800 m	2800 m	2800 m	3492 m	3492 m	3492 m	3492 m
$\Delta X_{\min}$	600 m	600 m	600 m	600 m	600 m	600 m	600 m
ΔF_{sh}	10	10	10	40	40	40	40
ΔF_{dp}	30	30	30	60	60	60	60
SLI	350 m	400 m	500 m	320 m	360 m	400 m	400 m
RLI	400 m	350 m	300 m	320 m	320 m	320 m	280 m
M_i	6	5	4	8	7	8	6
M_x	5	6	7	8	9	7	10
M	30	30	28	64	63	56	60
$X_{\min}$	532 m	532 m	583 m	453 m	482 m	512 m	488 m
$X_{\max,i}$	2100 m	2000 m	2000 m	2560 m	2520 m	3200 m	2400 m
$X_{\max,x}$	2000 m	2100 m	2100 m	2560 m	2880 m	2240 m	2800 m
F_{sh}	8.8	8.8	8.2	40.7	36.2	32.4	37.2
F_{dp}	29.9	29.9	27.9	63.8	62.0	54.5	59.5
LUG cost	0.040	0.040	0.488	0.065	0.085	0.312	0.251
MKB cost	21232	20071	18301	31170	29255	27131	28039

Discussion. The designs found with the LUG and the MKB methods depend on a large number of variables. In the first place target values have to be specified for various geophysical parameters. There is always some degree of uncertainty associated with those target values. The uncertainty can be expressed by allowing some percentage deviation from the target values. Yet, this means that the solution found by the Excel Solver is subject to uncertainties as well. Often, small variations in the problem description may lead to equally satisfactory but different solutions. The different solutions listed in Table 2 bear this out. The Excel spreadsheet is also useful for tweaking the parameters by hand without using the Solver. Changing one of the four integer decision variables to the next higher or lower integer gives immediate insight into the sensitivity of the cost function on the parameter choice.

The merit of the MKB method is not that it provides an accurate cost estimate of different acquisition geometries. The cost structure for different contractors will be different and is difficult to capture in a simple problem description as discussed here. Moreover, the data corresponding to the one-line crossline roll assumed in this paper may also be acquired in more cost-effective ways using different acquisition techniques (Vermeer, 2002). Yet, the MKB method can provide a quick alternative solution for situations where shots are known to be more expensive than receivers.

Conclusions. In this paper the survey design optimization methods proposed by Liner et al. (1999) and by Morrice et al. (2001) have been improved and combined into a single spreadsheet method. The concise description of the one-line roll orthogonal geometry with two equal station spacings and four integers (corresponding to shot line interval, receiver line interval, maximum inline offset, and maximum crossline offset) reduces the number of possible parameter choices considerably and allows the Excel Solver to produce fully satisfactory solutions at one click of the mouse. The combined

use of the two methods allows a quick comparison between alternative solutions, also in relation to survey cost.

Final remark. The Excel spreadsheet discussed in this paper is included on the CD-Rom enclosed in Vermeer (2002). A free copy may also be obtained by sending an e-mail to the author.

Suggested reading. "Practical aspects of 3D coherent noise filtering using (f-kx-ky) or wavelet transform filters" by Galibert et al. (SEG 2002 *Expanded Abstracts*). "From acquisition footprints to true amplitude" by Gesbert (*Geophysics*, 2002). "Contribution of new technologies and methods for 3D land seismic acquisition and processing applied to reservoir structure enhancement – Block 10, Yemen" by Girard et al. (SEG 2002 *Expanded Abstracts*). "3D seismic survey design" by Hornman et al. (*First Break*, 2000). "Use of recent advances in 3D land processing: a case history from the Pakistan Badin area" by Karagůl et al. (EAGE 2003 *Extended Abstracts*). "3-D seismic survey design as an optimization problem" by Liner et al. (SEG 1998 *Expanded Abstracts*). "3-D seismic survey design as an optimization problem" by Liner et al. (*The Leading Edge*, 1999). "Optimizing operations in 3-D land seismic surveys" by Morrice et al. (*Geophysics*, 2001). "3-D seismic survey design" by Vermeer (SEG, 2002).

Corresponding author: gijs-at-3dsymsam.nl

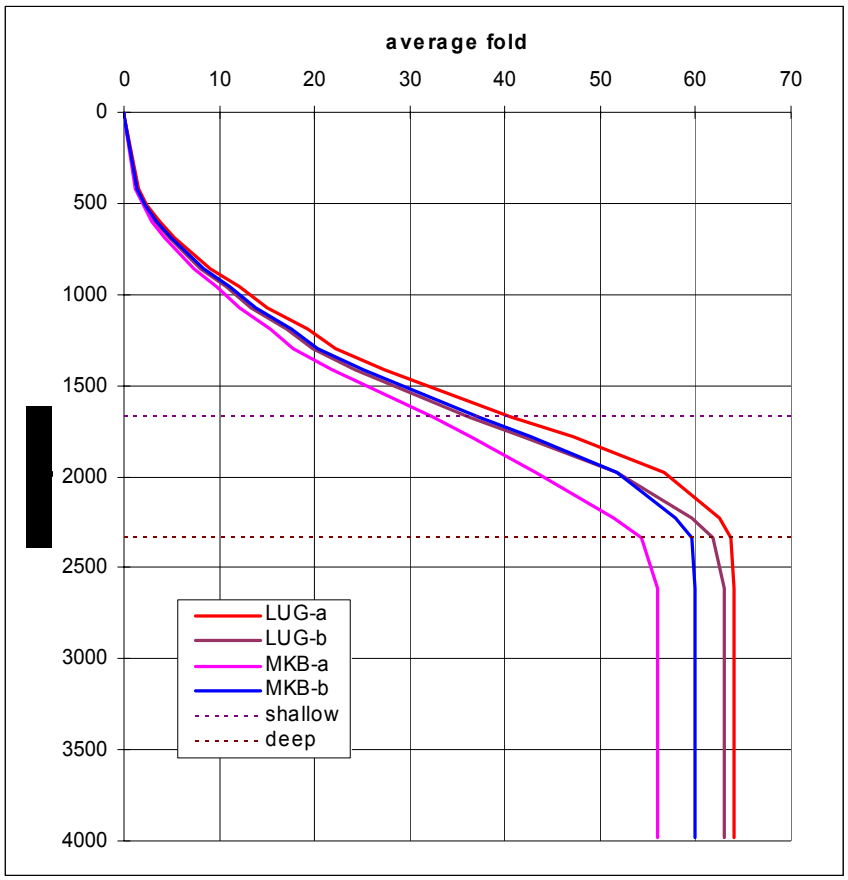

Figure 4. Average fold as function of two-way time for four different optimized solutions to the same design problem (Example 2 in Table 2). LUG-b and MKB-b are the optimal solutions found by using tighter constraints on F_{dp} than used for LUG-a and MKB-a. The levels of the shallow and the deep targets are indicated with horizontal dashed lines.